

# MIDAS: Modeling Ground-Truth Distributions with Dark Knowledge for Domain Generalized Stereo Matching

Peng Xu Zhiyu Xiang\* Jingyun Fu Tianyu Pu Hanzhi Zhong Eryun Liu  
College of Information Science and Electronic Engineering, Zhejiang University  
{xxxupeng, xiangzy, fujingyun, 3190105835, zhonghanzhi, eryunliu}@zju.edu.cn

## Abstract

Despite the significant advances in domain generalized stereo matching, existing methods still exhibit domain-specific preferences when transferring from synthetic to real domains, hindering their practical applications in complex and diverse scenarios. The probability distributions predicted by the stereo network naturally encode rich similarity and uncertainty information. Inspired by this observation, we propose to extract these two types of dark knowledge from the pre-trained network to model intuitive multi-modal ground-truth distributions for both edge and non-edge regions. To mitigate the inherent domain preferences of a single network, we adopt network ensemble and further distinguish between objective and biased knowledge in the Laplace parameter space. Finally, the objective knowledge and the original disparity labels are jointly modeled as a mixture of Laplacians to provide fine-grained supervision for the stereo network training. Extensive experiments demonstrate that: 1) Our method is generic and effectively improves the generalization of existing networks. 2) PCWNet with our method achieves the state-of-the-art generalization performance on both KITTI 2015 and 2012 datasets. 3) Our method outperforms existing methods in comprehensive ranking across four popular real-world datasets. Our code will be made available upon paper acceptance.

## 1. Introduction

Stereo matching plays a crucial role in numerous vision-based applications, including automatic driving, augmented reality, and robotics. For these safety-critical systems, ensuring the reliability of stereo networks in complex real-world scenarios is of paramount importance. Different from monocular depth estimation [41], collecting massive amounts of labeled or even unlabeled real data to train a stereo foundation model is extremely challenging due to the

\*Corresponding author.

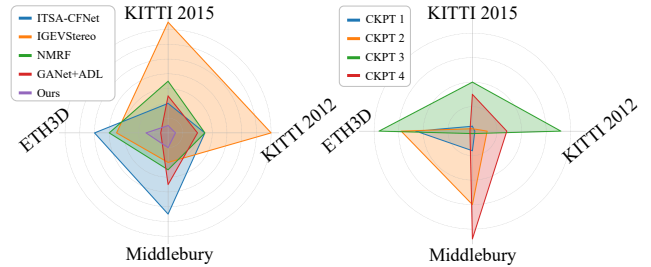


Figure 1. **Cross-domain preferences** of different network architectures (left) and different checkpoints of the same network [40] (right). All the methods are trained on synthetic dataset [27] and evaluated on four real-world datasets [11, 28, 30, 31]. The closer to the center, the better the performance.

hardware limitations. Existing works [2, 8, 24, 40, 46] attempt to directly train well-generalizing stereo networks in the synthetic domain [27] and have achieved considerable progress.

Nevertheless, these methods still exhibit undesired cross-domain preferences. As shown in Fig. 1 (left), ITSA-CFNet [8] performs well on KITTI 2015 [28] and 2012 [11] but poorly on Middlebury [30] and ETH3D [31], while IGEVStereo [39] is just the opposite. Rao *et al.* [29] point out that existing works typically report the optimal result among all checkpoints for each dataset separately. This conflicts with the practical demands, where a single network with fixed weights must maintain robust performance across diverse scenarios. Motivated by these limitations, our work aims to mitigate the domain preferences and improve the comprehensive generalization of a single checkpoint.

Guiding stereo networks to learn fine-grained disparity distributions has been proven effective in enhancing cross-domain generalization. Currently, the stereo ground-truth is usually modeled as the uni-modal Laplacian or Gaussian distribution, centered around the disparity label [3, 36, 49]. Xu *et al.* [40] model the multi-modal ground-truth distributions for edge regions but retain uni-modal modeling for non-edge regions, which limits their ability to address repetitive- or weak-textured regions. Fig. 1 (right) demon-

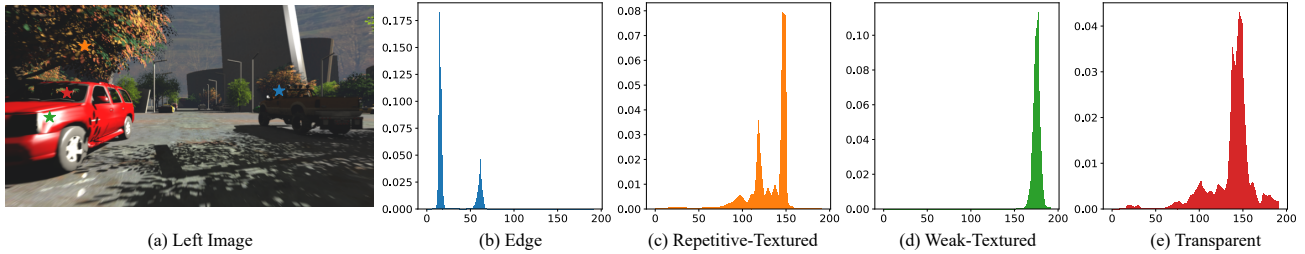


Figure 2. **Visualization of the probability distributions** output by PSMNet [1], trained with uni-modal Laplacian cross-entropy loss [36]. Four representative pixels (marked with colored stars in the left image) illustrate different distribution patterns. The stereo network naturally produces multi-modal distributions in edge  $\star$ , repetitive-textured  $\star$ , and transparent  $\star$  regions, while generating wider uni-modal distribution in weak-textured  $\star$  region.

strates that their different checkpoints also exhibit varying domain preferences.

Our exploration stems from the observation that stereo matching networks naturally output multi-modal distributions not only in edge region but also in non-edge regions with repetitive textures or transparent surfaces, as shown in Fig. 2. These multi-modal distributions in stereo matching are analogous to the multi-hot distributions in classification task [17], with both encoding the similarity information. However, stereo matching differs from classification in the distribution patterns. While classification networks produce responses characterized by Dirac delta functions at discrete class locations, stereo matching networks generate modes with finite width for each correspondence candidate. This width encodes valuable uncertainty information about the pixel-wise matching process. When matching becomes highly uncertain, stereo networks output the wider modes, as shown in Fig. 2 (d).

Building upon the insights into the properties of stereo distributions, we propose to extract dark knowledge (similarity and uncertainty) from the pre-trained stereo network to model informative ground-truth distributions for both edge and non-edge regions. We adopt network ensemble [21, 37, 43] to mitigate the domain preferences inherent in a single pre-trained network. However, naïvely superimposing the outputs from the ensemble fails to effectively fuse the uncertainty information and compromises the uni-modal nature of each mode. To address these problems, we innovatively aggregate the dark knowledge in the Laplace parameter space. Specifically, we first separate individual modes from the output multi-modal distributions and project them as a series of points in the Laplace parameter space. Then, we cluster these points to distinguish the objective knowledge (effective clusters) from the biased knowledge (noise). Finally, the objective knowledge, together with the disparity labels, is utilized to construct the multi-modal ground-truth distributions.

We conduct extensive experiments to demonstrate the effectiveness of our method on PSMNet [1], GwcNet [14], and PCWNet [33]. At the time of writing this paper,

PCWNet with our method achieves the state-of-the-art generalization performance among all published methods on both KITTI 2015 [28] and 2012 [11] datasets. For a more intuitive comparison of comprehensive generalization performance, we compute the mean rank across four real-world datasets [11, 28, 30, 31]. PCWNet with our method also outperforms the existing methods.

Our contributions can be summarized as follows:

- To the best of our knowledge, we are the first to model multi-modal ground-truth distributions for all regions in stereo matching. By incorporating texture information into modeling, we provide more intuitive and insightful supervision signals for network learning.
- We propose to aggregate objective knowledge in the Laplace parameter space, reducing the introduction of biased knowledge during the modeling process.
- We achieve the state-of-the-art cross-domain generalization performance on KITTI 2015 and 2012 datasets, and rank 1<sup>st</sup> in the comprehensive comparison across four popular real-world datasets.
- Our method achieves stable cross-domain generalization across multiple datasets with the fixed checkpoint and demonstrates superior robustness when handling various challenging regions, significantly enhancing the reliability of stereo vision systems in real-world applications.

## 2. Related Work

**Deep Stereo Matching.** In recent years, deep learning-based stereo matching methods have become mainstream and achieve performance far exceeding traditional methods. DispNet [27] is the first end-to-end stereo network. GCNet [20] aggregates information through 3D convolution. PSMNet [1] and GwcNet [14] are the two most popular stereo backbones [4, 8, 24, 35, 38, 40, 48, 49], prompting the prosperity of the community. The former improves the extracted features through spatial pyramid pooling [15], while the latter preserves feature similarity information in the cost volume through the group-wise correlation. Besides the cost volume filtering-based methods mentioned above, iterative optimization-based meth-

ods [6, 19, 22, 23, 39, 50] show impressive results. Following RAFT [34], these methods adopt ConvGRUs [7] to update the disparity map recurrently and bypass the computational burden of 3D convolutions, making high-resolution stereo matching possible. IGEVStereo [39] further provides a better initial disparity map for the updater with a tiny 3D convolution network. MoCha-Stereo [6] achieves accurate detail matching by capturing repeated geometric contours with the motif [42] channel attention mechanism.

**Cross-Domain Generalization.** Stereo networks that can generalize well from synthetic to real domains are promising. DSMNet [46] designs a domain normalization layer and a non-local graph-based filtering layer to reduce the domain shifts. ITSA [8] bridges the gap between the extracted features from original and perturbed images to minimize the feature representation sensitivity. GraftNet [24] exploits a pre-trained encoder to extract broad-spectrum features and compresses features for better matching. FCNet [48] introduces a contrastive feature loss and a selective whitening loss to maintain the feature consistency. PCWNet [33] fuses the multi-scale volumes to extract domain-invariant features, and narrows the residue searching range for easier matching. Chang *et al.* [2] transform the training samples into new domains with diverse distributions and minimize the cross-domain feature inconsistency to capture domain-invariant features.

**Ground-truth Distribution Modeling.** Unlike classification, the ground-truth distribution of stereo matching cannot be modeled as a one-hot vector due to the conflict between the discrete disparity candidates and the continuous disparity label. PDSNet [36] proposes to model the ground-truth distributions as discrete Laplacians with fixed width and infer the final disparity with a maximum a posteriori estimator. Chen *et al.* [3] model the distribution as the discrete Gaussian and determine the scope of the major mode based on monotonicity during inference. AcfNet [49] models uncertainty by computing the variances of the output distributions. Xu *et al.* [40] achieve outstanding generalization performance by embedding edge information into the ground-truth modeling and optimizing the selection strategy of the major mode. Following these studies, our goal is to develop a better ground-truth modeling for stereo matching.

**Knowledge Distillation.** The concept of knowledge distillation was first proposed by Hinton *et al.* in [17]. The core idea is to use the dark knowledge (*i.e.*, soft labels) from a teacher network to train a student network. By leveraging the soft labels, the student network gains insights into the similarity between classes, leading to improved generalization on unseen domains. Subsequently, the concept of dark knowledge has been continuously enriched, including attention maps [44], activation boundary [16], relationship graph [26], *etc.* Additionally, the student can access a wider range of knowledge by aggregating the outputs from a net-

work ensemble [21, 37, 43]. Despite the widespread use of dark knowledge in classification and segmentation, it remains largely unexplored in stereo matching. In this paper, we focus on extracting dark knowledge from the pre-trained ensemble to construct multi-modal probability distributions to train a domain generalized stereo network.

## 3. Method

### 3.1. Preliminary

Stereo matching networks based on the cost volume filtering strategy [1, 14, 20, 33] output a discrete probability distribution  $\mathbf{p} = [p_0, p_1, \dots, p_{D-1}] \in \mathbb{R}^{1 \times D}$  for each pixel of the target image, where  $D$  is the pre-defined disparity search range. Treating stereo matching as a classification task [35, 36, 40, 49], the output distribution can naturally be supervised by the cross-entropy loss:

$$\mathcal{L}_{ce}(\mathbf{p}, \hat{\mathbf{p}}) = - \sum_{d=0}^{D-1} \hat{p}_d \cdot \log p_d \quad (1)$$

where  $\hat{\mathbf{p}} = [\hat{p}_0, \hat{p}_1, \dots, \hat{p}_{D-1}]$  is the ground-truth distribution. The core problem is that  $\hat{\mathbf{p}}$  remains unknown, as the disparity labels  $\hat{d}$  in stereo matching are continuous scalars obtained from depth sensors such as LiDAR. Several studies [3, 36] model the ground-truth distribution as a unimodal distribution, of which the mean value is set to the disparity label. Later, Xu *et al.* [40] demonstrate that the multi-modal distribution is more natural than the naïve unimodal distribution at the edge and can provide better supervision signals. Considering the lack of exploration of non-edge regions in existing research, we aim to develop a reasonable and effective ground-truth modeling method for all regions in stereo matching.

Manually matching similar textures between stereo image pairs to model multi-modal distributions for non-edge regions is exhausting and infeasible. We observe that stereo networks typically output multi-modal distributions not only in edge regions but also in repetitive-textured or transparent regions, and produce wider modes in weak-textured regions, as shown in Fig. 2. Multiple modes indicate multiple similar matches in the reference image, while wider modes reflect greater matching uncertainty. Therefore, we leverage these two types of dark knowledge to model ground-truth distributions for both edge and non-edge regions. Our method enriches the information within the ground-truth distribution, enabling stereo networks to learn more knowledge from the training samples.

### 3.2. MIDAS

In this section, we introduce how to extract dark knowledge from the pre-trained stereo networks, and leverage it to construct our multi-modal ground-truth distribution.

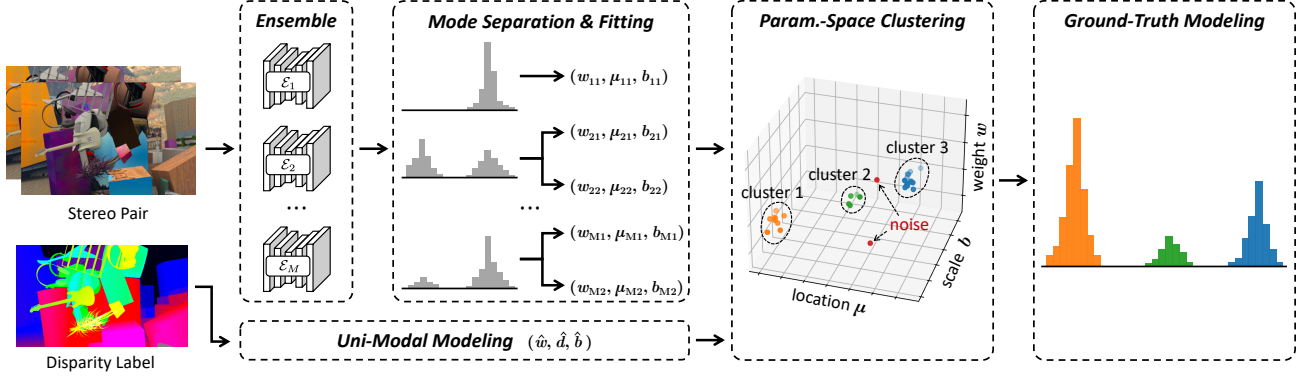


Figure 3. **Illustration of the ground-truth distribution modeling.** For each pixel in the input image pair, the network ensemble predicts  $M$  multi-modal probability distributions. Individual modes are separated from these distributions and fitted as parameterized Laplacians  $(w, \mu, b)$ . The disparity label is also modeled as the uni-modal Laplacian with coordinate  $(\hat{w}, \hat{d}, \hat{b})$ . Then, we cluster these modes in the parameter space to distinguish the objective knowledge (effective clusters) from the biased knowledge (noise). The elements within each cluster are fused and modeled as a formulated mode in the final ground-truth distribution.

As shown in Fig. 3, given a stereo image pair, the pre-trained network ensemble  $\{\mathcal{E}_1, \mathcal{E}_2, \dots, \mathcal{E}_M\}$  outputs a set of probability distributions  $\{\mathbf{p}_1, \mathbf{p}_2, \dots, \mathbf{p}_M\}$  for each pixel in the target image. Then, we separate modes from the output distribution, and fit each mode as a discrete Laplacian:

$$\text{Laplacian}(\mathbf{d}; w, \mu, b) = w \cdot \frac{\exp(-\frac{|\mathbf{d}-\mu|}{b})}{\sum_{d \in \mathbf{d}} \exp(-\frac{|d-\mu|}{b})} \quad (2)$$

where  $\mathbf{d} = [0, 1, \dots, D-1]$  is the disparity candidates. Specifically, the weight parameter  $w$  is defined as the sum of the probabilities within the mode. We apply soft-argmin [20] and mean absolute deviation (MAD) [9] operations upon the normalized mode to compute the location parameter  $\mu$  and the scale parameter  $b$  in Eq. (2), respectively. The details are shown in Algorithm 1. In this way, we transform the predicted distribution to a set of points  $\mathcal{T} = \{(w, \mu, b)\}$  in the Laplace parameter space. The number of elements in  $\mathcal{T}$  indicates the number of modes in the distribution.  $\mu$  denotes the center location of each mode, representing the potential disparity.  $w$  denotes the matching probability of each mode, reflecting the degree of similarity between modes.  $b$  denotes the width of each mode, reflecting the strength of the texture information in the corresponding region. To mitigate the impact of all pre-trained networks making incorrect predictions simultaneously, we additionally add a uni-modal Laplacian distribution centered around the disparity label  $\hat{d}$ , *i.e.*, a point with coordinate  $(\hat{w}, \hat{d}, \hat{b})$ , to the Laplace parameter space.

Next, we apply the DBScan algorithm [10] to perform clustering along the  $\mu$ -axis, resulting in  $K$  clusters  $\{C_1, C_2, \dots, C_K\}$  and a set of noise. Note that even when the label point  $(\hat{w}, \hat{d}, \hat{b})$  has no adjacent points, we still consider it as an effective cluster rather than noise. The points within each cluster have similar location parameters, indicating that a significant number of pre-trained networks re-

---

#### Algorithm 1 Mode Separation and Fitting

---

**Input:** probability distribution  $\mathbf{p}$   
**Input:** threshold  $\epsilon > 0, \sigma > 0$   
**Output:** a set of triples  $\mathcal{T}$

```

 $\mathcal{T} \leftarrow \emptyset$ 
while  $\max(\mathbf{p}) > \epsilon$  do
   $l, r \leftarrow \text{argmax}(\mathbf{p})$ 
  while  $\mathbf{p}[l] - \mathbf{p}[l-1] > \sigma$  and  $l-1 \geq 0$  do
     $l \leftarrow l-1$ 
  end while
  while  $\mathbf{p}[r] - \mathbf{p}[r+1] > \sigma$  and  $r+1 \leq D-1$  do
     $r \leftarrow r+1$ 
  end while
   $w \leftarrow \sum_{d=l}^r \mathbf{p}[d]$ 
   $\mu \leftarrow \sum_{d=l}^r (\mathbf{p}[d]/w) \cdot d$ 
   $b \leftarrow \sum_{d=l}^r (\mathbf{p}[d]/w) \cdot |d-\mu|$ 
   $\mathcal{T} \leftarrow \mathcal{T} \cup \{(w, \mu, b)\}$ 
   $\mathbf{p}[l:r] \leftarrow 0$ 
end while
Return  $\mathcal{T}$ 

```

---

spond to the similar disparity candidates. We believe that these points are reliable and represent the objective knowledge within the ensemble. Conversely, the noisy points correspond to the unreliable modes, which represent the biased knowledge. We remove this biased knowledge during modeling to generate better ground-truth distributions.

Finally, the stereo ground-truth distribution is modeled as a mixture of  $K$  Laplacians:

$$\begin{aligned} \hat{\mathbf{p}} &= \sum_{k=1}^K \text{Laplacian}(\mathbf{d}; w_k, \mu_k, b_k) \\ &= \sum_{k=1}^K w_k \cdot \frac{\exp(-\frac{|\mathbf{d}-\mu_k|}{b_k})}{\sum_{d \in \mathbf{d}} \exp(-\frac{|d-\mu_k|}{b_k})} \end{aligned} \quad (3)$$

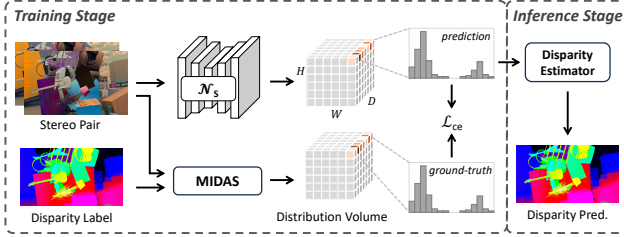


Figure 4. **Training and inference pipeline.**  $\mathcal{N}_s$ : the stereo network to be trained. MIDAS: the ground-truth distribution modeling method described in Sec. 3.2.

where  $w_k$ ,  $\mu_k$ , and  $b_k$  are the means of the weight, location, and scale parameters of elements in cluster  $C_k$ , respectively. Assuming that the label point is located in cluster  $C_1$ , we set  $\mu_1 = \hat{d}$ . In addition, the modeled distribution is normalized as  $\hat{\mathbf{p}}/\|\hat{\mathbf{p}}\|_1$  to ensure that the sum of probabilities is equal to one.

Our method offers the following advantages: 1) By clustering in the parameter space and filtering out noise, we effectively avoid introducing biased knowledge into the modeled ground-truth. 2) Directly superimposing the output distributions of the pre-trained ensemble may result in multiple peaks for the fused mode due to the misalignment of mode centers. In contrast, fusing modes in the parameter space and remodeling them as the Laplacian can maintain the uni-modal nature. 3) Our method can adaptively adjust the mode number in the ground-truth distribution as well as the height and width of each mode not only for edge regions but also for non-edge regions.

### 3.3. Overall Pipeline

Fig. 4 illustrates the overall pipeline of our method. To train a stereo network  $\mathcal{N}_s$ , the dark knowledge embedded multi-modal distributions described in Sec. 3.2 are applied as the ground-truth to supervise the predicted distributions of  $\mathcal{N}_s$ . Following [41], we apply color jittering and random occlusion only to the image pairs input to  $\mathcal{N}_s$  to encourage the trained network to acquire domain-invariant features. Cross-entropy loss encourages the stereo network to output multi-modal distributions [40]. Directly applying the weighted average operation (soft-argmin) [20] to regress disparity on the multi-modal distributions leads to over-smoothing artifacts [3], *i.e.* the disparity is incorrectly estimated between modes. For this reason, we employ DME [40] instead of soft-argmin to estimate the final disparities from the predicted distributions during inference.

## 4. Experiments

### 4.1. Datasets and Evaluation Metrics

Following previous works [8, 46, 48], we train stereo networks on SceneFlow [27] and evaluate cross-domain gen-

eralization performance on the training sets of four real-world datasets: KITTI 2015 [28], KITTI 2012 [11], Middlebury [30], and ETH3D [31].

SceneFlow is a synthetic dataset that includes 35,454 pairs of stereo images for training and 4,370 pairs for testing. We use its *finalpass* training set, as it considers motion blur and depth of field, making it more realistic and challenging. KITTI 2012 and 2015 are two driving scene datasets, including 194 and 200 training pairs respectively. Middlebury and ETH3D are small datasets, both containing dozens of real image pairs.

We employ  $kpx$  as the performance metric, which counts the percentage of valid pixels with an absolute disparity error greater than the threshold  $k$ . For KITTI 2015 and 2012, the threshold is set to 3. For ETH3D, the threshold is set to 1. For Middlebury, we evaluate on its half resolution training set and set the threshold to 2.

### 4.2. Implementation Details

We perform experiments on PSMNet [1] and GwcNet [14], two classic networks frequently employed as backbones, along with PCWNet [33], which is designed for the cross-domain generalization. We first pre-train these networks with uni-modal Laplacian cross-entropy loss [36], and select three checkpoints from each network to form the ensemble for generating the multi-modal ground-truth distributions.  $\hat{w}$  is set to 1 and  $\hat{b}$  is set to 0.8.  $\epsilon$  and  $\sigma$  in Algorithm 1 are all set to  $1 \times 10^{-3}$ . The distance threshold and the density threshold in DBScan algorithm [10] are set to 3 and 2, respectively. Then, we train these three networks with our modeled ground-truth from scratch. For all experiments, we train the stereo networks on a single NVIDIA 4090 GPU for 80 epochs. We apply Adam ( $\beta_1 = 0.9$  and  $\beta_2 = 0.999$ ) to optimize the networks and one-cycle schedule ( $max\_lr = 1 \times 10^{-3}$ ) to adjust the learning rate.

### 4.3. Cross-Domain Evaluation

**Comparison with state-of-the-art.** As shown in Tab. 1, all three backbones [1, 14, 33] trained with our method demonstrate promising generalization performance. In particular, PCWNet [33] with our method achieves state-of-the-art cross-domain generalization performance on most datasets. Compared to the baseline, it yields considerable improvements of 29.29%, 15.00%, 54.34%, and 47.69% on KITTI 2015 [28], KITTI 2012 [11], Middlebury [30], and ETH3D [31], respectively. These results prove that stereo networks supervised by our multi-modal ground-truth distributions can effectively learn generalizable matching principles from synthetic data and transfer well to real-world scenarios.

We further compute the mean rank to compare the comprehensive generalization performance of the listed methods across diverse scenarios. As shown in Tab. 1,

Method	Publication	KITTI 2015 >3px	KITTI 2012 >3px	Middlebury >2px	ETH3D >1px	Mean Rank
PSMNet [1]	CVPR 2018	16.30 <sup>18</sup>	15.10 <sup>18</sup>	25.10 <sup>18</sup>	23.80 <sup>18</sup>	18.00
GwcNet [14]	CVPR 2018	12.80 <sup>17</sup>	11.70 <sup>17</sup>	18.10 <sup>16</sup>	9.00 <sup>16</sup>	16.50
GANet [45]	CVPR 2019	11.70 <sup>16</sup>	10.10 <sup>16</sup>	20.30 <sup>17</sup>	14.10 <sup>17</sup>	16.5
DSMNet [46]	ECCV 2020	6.50 <sup>15</sup>	6.20 <sup>15</sup>	13.80 <sup>13</sup>	6.20 <sup>14</sup>	14.25
CFNet [32]	CVPR 2021	5.80 <sup>12</sup>	4.70 <sup>11</sup>	15.30 <sup>14</sup>	5.80 <sup>12</sup>	12.25
Mask-CFNet [29]	CVPR 2023	5.80 <sup>12</sup>	4.80 <sup>12</sup>	13.70 <sup>12</sup>	5.70 <sup>11</sup>	11.75
Raft-Stereo [23]	3DV 2021	5.70 <sup>11</sup>	5.20 <sup>14</sup>	12.60 <sup>11</sup>	3.30 <sup>6</sup>	10.50
FC-GANet [48]	CVPR 2022	5.30 <sup>9</sup>	4.60 <sup>10</sup>	10.20 <sup>9</sup>	5.80 <sup>12</sup>	10.00
PCWNet [33]	ECCV 2022	5.60 <sup>10</sup>	4.20 <sup>5</sup>	15.77 <sup>15</sup>	5.20 <sup>10</sup>	10.00
IGEV-Stereo [39]	CVPR 2023	6.03 <sup>14</sup>	5.18 <sup>13</sup>	7.27 <sup>3</sup>	3.60 <sup>7</sup>	9.25
Graft-GANet [24]	CVPR 2022	4.90 <sup>6</sup>	4.20 <sup>5</sup>	9.80 <sup>8</sup>	6.20 <sup>14</sup>	8.25
ITSA-CFNet [8]	CVPR 2022	4.70 <sup>4</sup>	4.20 <sup>5</sup>	10.40 <sup>10</sup>	5.10 <sup>9</sup>	7.00
StereoRisk [25]	ICML 2024	5.19 <sup>8</sup>	4.43 <sup>9</sup>	9.32 <sup>7</sup>	2.41 <sup>2</sup>	6.50
NMRF [13]	CVPR 2024	5.10 <sup>7</sup>	4.20 <sup>5</sup>	7.50 <sup>4</sup>	3.80 <sup>8</sup>	6.00
GANet + ADL [40]	CVPR 2024	4.84 <sup>5</sup>	3.93 <sup>4</sup>	8.72 <sup>6</sup>	2.31 <sup>1</sup>	4.00
PSMNet + Ours	—	4.49 <sup>3</sup>	3.72 <sup>2</sup>	7.95 <sup>5</sup>	3.17 <sup>5</sup>	3.75
GwcNet + Ours	—	4.16 <sup>2</sup>	3.74 <sup>3</sup>	7.23 <sup>2</sup>	2.91 <sup>4</sup>	2.75
PCWNet + Ours	—	3.96 <sup>1</sup>	3.57 <sup>1</sup>	7.20 <sup>1</sup>	2.72 <sup>3</sup>	1.50

Table 1. **Quantitative evaluation of cross-domain generalization.** All methods are trained on SceneFlow [27] and evaluated on four popular real-world datasets [11, 28, 30, 31]. Mean rank is computed to compare the comprehensive generalization performance. The **best** and **second best** are marked with colors.

PCWNet [33] with our method rank first among all methods, followed by GwcNet [14] and PSMNet with our method. The superior comprehensive performance of our method highlights its potential in enhancing the reliability of stereo vision system.

**Comparison with ground-truth modeling.** In practical applications, stereo networks can only load a fixed checkpoint. Therefore, the generalization performance of a single checkpoint deserves special attention. We compare the single checkpoint performance of our method with both uni-modal [36] and multi-modal [40] ground-truth modeling methods. For each method, we select the best checkpoint among all its checkpoints, following the ranking strategy described in Tab. 1. As shown in Tab. 2, our single checkpoint performance (last row) even surpasses the best performance of ADL (third row) [40], which models the multi-modal distributions for edge regions only, on all datasets. We also report the degradation of the single checkpoint performance compared to the best performance on each dataset. The uni-modal method [36] and the edge-aware multi-modal method [40] degrade by 12.06% and 5.30% respectively, while our method only degrades by 2.81%. This further demonstrates the advantage of our method that models multi-modal distributions for both edge and non-edge regions.

We visualize the disparity maps to provide more intuitive comparisons with the modeling methods. As shown in Fig. 5, in weak-textured regions such as the sky (top

Method	KT15 >3px	KT12 >3px	MB >2px	ETH3D >1px	Average Degradation
UMCE [36]	4.73	4.64	9.76	4.18	
UMCE*	5.62 <sup>-18.82%</sup>	5.55 <sup>-19.61%</sup>	9.76 <sup>-0.00%</sup>	4.59 <sup>-9.81%</sup>	-12.06%
ADL [40]	4.78	4.23	8.85	3.44	
ADL*	4.78 <sup>-0.00%</sup>	4.23 <sup>-0.00%</sup>	8.95 <sup>-1.13%</sup>	4.13 <sup>-20.06%</sup>	-5.30%
Ours	<b>4.49</b>	<b>3.72</b>	<b>7.95</b>	<b>3.17</b>	
Ours*	<b>4.49<sup>-0.00%</sup></b>	<b>3.72<sup>-0.00%</sup></b>	8.29 <sup>-4.28%</sup>	3.39 <sup>-6.94%</sup>	<b>-2.81%</b>

Table 2. **Quantitative comparison with ground-truth modeling methods.** All methods are trained on PSMNet [1]. \*represents generalization performance from the optimal single checkpoint. We also report the performance degradation of the single checkpoint relative to the best result on each dataset, indicated by red subscripts.

row), both uni-modal [36] and multi-modal [40] methods result in large areas of artifacts, which are not accurately reflected in the metrics because the sky lacks disparity labels. The same phenomenon can be observed in the white areas of containers (second row). Our method also demonstrates superior performance in handling repetitive-textured regions, achieving smoother disparity for grass (third row) and avoiding mismatching the chair gaps (fifth row). Additionally, our method obtains sharp and accurate object edges (fourth row), which is crucial for downstream tasks such as 3D object detection [5], and exhibits considerable robustness when addressing the challenging case of strong glare (last row). These examples demonstrate that by mod-

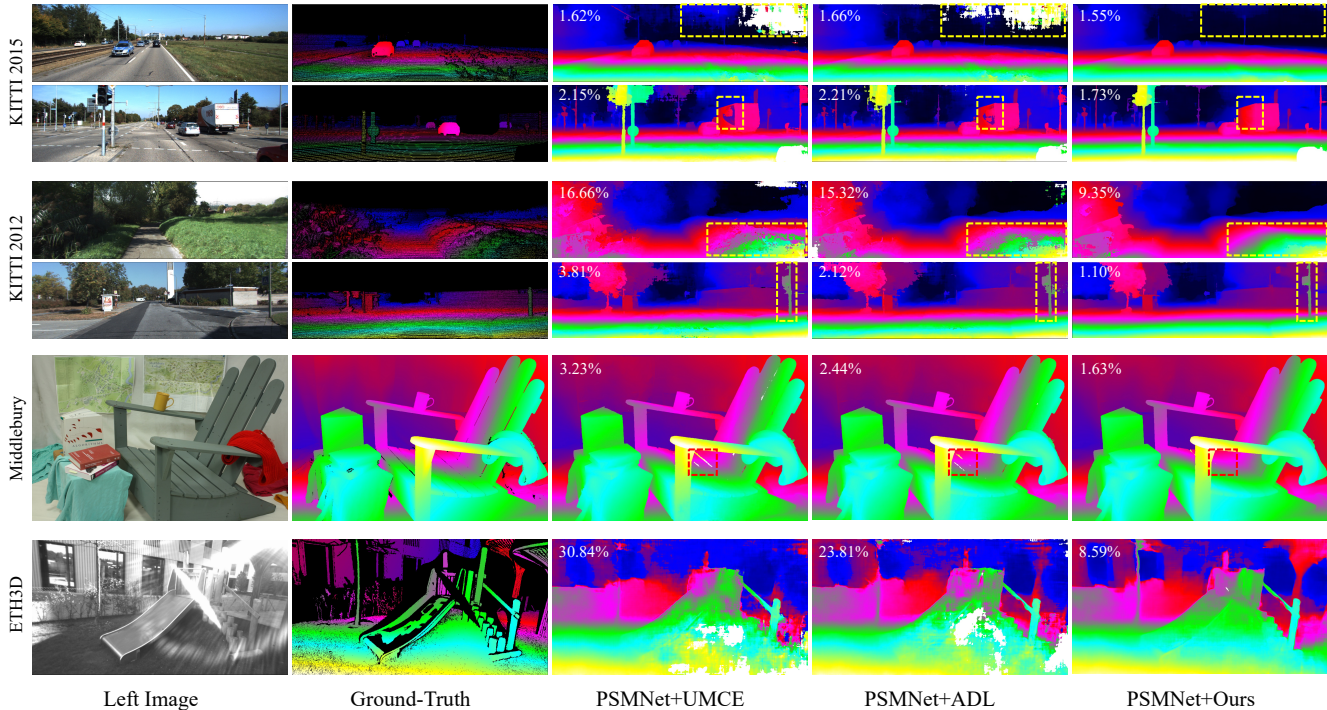


Figure 5. **Qualitative evaluation of cross-domain generalization.** All methods are trained on SceneFlow [27] and evaluated on four real-world datasets [11, 28, 30, 31]. Compared to uni-modal method (UMCE) [36] and edge-aware multi-modal method (ADL) [40], our method demonstrates superior performance in weak-textured regions (sky, container), repetitive-textured regions (grass, chair gaps), and object edges (sign post). Furthermore, our method exhibits excellent robustness when handling strong glare (last row). The outlier metric is displayed in the upper left corner of each disparity map.



Figure 6. **Qualitative evaluation of cross-domain generalization** on daily-life images from Holopix50k [18].

eling the ground-truth distributions as multi-modal distributions for both edge and non-edge regions and adaptively adjusting the width of each mode, our method successfully guides stereo networks to learn matching similarity and uncertainty to cope with real-world complexities. Fig. 6 shows more qualitative results of our method on daily-life images of Holopix50k [18].

**Comparison with knowledge distillation.** As shown in Tab. 3, compared with the vanilla knowledge distilla-

Method	KT15	KT12	MB	ETH3D
KD [17]	4.67	4.41	9.00	4.02
Average [43]	4.58	3.96	8.61	3.53
Entropy [21]	4.61	4.10	8.29	3.71
Confidence [47]	4.54	3.78	7.58	3.75
Ours	4.49	3.72	7.95	3.17

Table 3. **Quantitative comparison with knowledge distillation methods.** Beside the vanilla distillation [17], we evaluate three ensemble methods that employ average [43], entropy-based [21], and confidence-aware [47] fusion strategies, respectively. All methods are trained on PSMNet [1].

tion [17], ensemble methods [21, 43, 47] aggregate the output distributions of multiple pre-trained networks and effectively improve the generalization of stereo networks. Our method achieves further generalization improvement on most datasets, which we attribute to our fusion strategy for dark knowledge. Simply superimposing the predicted distributions introduces the noisy modes and compromises the uni-modal nature of each mode due to the misalignment of the mode centers. We propose to fuse modes in the parameter space and remodel the aggregated clusters as

Method	PSMNet [1]	PCWNet [33]	GwcNet [14]	IGEVStereo [39]	ICGNet [12]	GANet+ADL [40]	PCWNet+Ours
>3px	4.56	3.68	3.30	2.47	2.34	<b>1.81</b>	2.03

Table 4. **Quantitative evaluation on SceneFlow test set [27]**. We report the percentage of outliers with the absolute error larger than 3px.

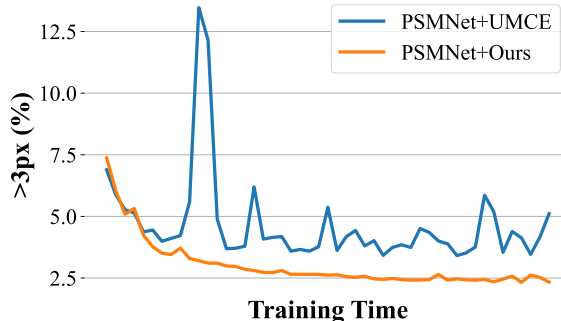


Figure 7. **Visualization of outlier rate curves** during training on SceneFlow test set [27]. We report the percentage of outliers with the absolute error larger than 3px.

Laplacians, making the ground-truth distribution better formulated and easier to learn.

#### 4.4. In-Domain Evaluation

**Comparison with state-of-the-art.** Although our method primarily focuses on the cross-domain generalization, it still achieves competitive performance in the source domain [27], as shown in Tab. 4. PCWNet [33] with our method generates only 2.03% outliers, representing a 44.84% improvement over the baseline. Both ADL [40] and our method outperform competitors trained with L1 loss. This is attributed to the finer-grained supervision signals provided by the modeled distributions compared to the original disparity labels, enabling the stereo networks to learn more efficiently.

**Convergence stability.** To further investigate the impact of different ground-truth distributions on stereo network learning, we plot the outlier rate curves during training on SceneFlow test set [27]. As illustrated in Fig. 7, our method achieves more stable and better convergence compared to the uni-modal method [36]. The stereo network effectively learns valuable dark knowledge from our proposed multi-modal ground-truth distributions, thereby reducing overfitting to the training set.

#### 4.5. Ablation Study

Tab. 5 presents the ablation study on the number of network architectures and checkpoints in the pre-trained ensemble. Our methods (second block) consistently outperform the modeling method (first row) [1] and the distillation method (second row) [17]. Compared to ensembling different architectures, ensembling different checkpoints helps mitigate training randomness and achieves better general-

#Arch.	#CKPT	KT15	KT12	MB	ETH3D
0	0	4.73	4.64	9.76	4.18
1	1	4.67	4.41	9.00	4.02
1	2	4.57	3.87	8.47	3.34
2	1	4.64	3.89	8.27	3.64
2	2	4.59	3.82	8.01	3.40
3	3	<b>4.49</b>	<b>3.72</b>	<b>7.95</b>	<b>3.17</b>

Table 5. **Ablation study** of the number of network architectures and checkpoints in the pre-trained ensemble. All methods are trained on PSMNet [1].

Method	KT15	KT12	MB	ETH3D
PSMNet [1] + Ours	<b>4.49</b>	<b>3.72</b>	<b>7.95</b>	<b>3.17</b>
w/o BKF	4.57	3.81	8.47	3.40

Table 6. **Ablation study** of biased knowledge filtering (BKF).

ization performance. Increasing the number of architectures and checkpoints yields further improvements in generalization. Due to computational resource constraints, we do not ablate larger-scale ensembles, which we believe could still achieve some level of performance improvement.

We also perform an ablation study to verify the effectiveness of filtering biased knowledge. As shown in Tab. 6, the preservation of noisy points clustered in the Laplace parameter space leads to poorer generalization performance across all datasets, demonstrating that these points are indeed detrimental to network learning.

## 5. Conclusion

In this paper, we present MIDAS, a novel method that extracts similarity and uncertainty information from the pre-trained network to model ground-truth distributions for stereo matching. To mitigate the impact of domain preferences in a single network, we employ the network ensemble. Specifically, we propose to aggregate objective knowledge in the Laplace parameter space and ultimately model the ground-truth distribution as a mixture of Laplacians. Our method effectively improves the generalization performance of cost volume filtering-based stereo networks. By modeling intuitive patterns for both edge and non-edge regions, our method exhibits considerable robustness in handling real-world challenges. Last but not least, our single checkpoint network achieves stable generalization performance across diverse scenarios, satisfying the practical demands of real-world applications.

## References

- [1] Jia-Ren Chang and Yong-Sheng Chen. Pyramid stereo matching network. In *Proceedings of the IEEE conference on computer vision and pattern recognition*, pages 5410–5418, 2018. 2, 3, 5, 6, 7, 8
- [2] Tianyu Chang, Xun Yang, Tianzhu Zhang, and Meng Wang. Domain generalized stereo matching via hierarchical visual transformation. In *Proceedings of the IEEE/CVF Conference on Computer Vision and Pattern Recognition*, pages 9559–9568, 2023. 1, 3
- [3] Chuangrong Chen, Xiaozhi Chen, and Hui Cheng. On the over-smoothing problem of cnn based disparity estimation. In *Proceedings of the IEEE/CVF International Conference on Computer Vision*, pages 8997–9005, 2019. 1, 3, 5
- [4] Shuya Chen, Zhiyu Xiang, Peng Xu, and Xijun Zhao. A normalized disparity loss for stereo matching networks. *IEEE Robotics and Automation Letters*, 8(1):33–40, 2022. 2
- [5] Yilun Chen, Shu Liu, Xiaoyong Shen, and Jiaya Jia. Dsgn: Deep stereo geometry network for 3d object detection. In *Proceedings of the IEEE/CVF conference on computer vision and pattern recognition*, pages 12536–12545, 2020. 6
- [6] Ziyang Chen, Wei Long, He Yao, Yongjun Zhang, Bingshu Wang, Yongbin Qin, and Jia Wu. Mocha-stereo: Motif channel attention network for stereo matching. In *Proceedings of the IEEE/CVF Conference on Computer Vision and Pattern Recognition*, pages 27768–27777, 2024. 3
- [7] Kyunghyun Cho, Bart Van Merriënboer, Caglar Gulcehre, Dzmitry Bahdanau, Fethi Bougares, Holger Schwenk, and Yoshua Bengio. Learning phrase representations using rnn encoder-decoder for statistical machine translation. *arXiv preprint arXiv:1406.1078*, 2014. 3
- [8] WeiQin Chuah, Ruwan Tennakoon, Reza Hoseinnezhad, Alireza Bab-Hadiashar, and David Suter. Itsa: An information-theoretic approach to automatic shortcut avoidance and domain generalization in stereo matching networks. In *Proceedings of the IEEE/CVF Conference on Computer Vision and Pattern Recognition*, pages 13022–13032, 2022. 1, 2, 3, 5, 6
- [9] KMT Elsayed. Mean absolute deviation: analysis and applications. *International Journal of Business and Statistical Analysis*, 2(02), 2015. 4
- [10] Martin Ester, Hans-Peter Kriegel, Jörg Sander, Xiaowei Xu, et al. A density-based algorithm for discovering clusters in large spatial databases with noise. In *kdd*, pages 226–231, 1996. 4, 5
- [11] Andreas Geiger, Philip Lenz, and Raquel Urtasun. Are we ready for autonomous driving? the kitti vision benchmark suite. In *2012 IEEE conference on computer vision and pattern recognition*, pages 3354–3361. IEEE, 2012. 1, 2, 5, 6, 7
- [12] Rui Gong, Weide Liu, Zaiwang Gu, Xulei Yang, and Jun Cheng. Learning intra-view and cross-view geometric knowledge for stereo matching. In *Proceedings of the IEEE/CVF Conference on Computer Vision and Pattern Recognition*, pages 20752–20762, 2024. 8
- [13] Tongfan Guan, Chen Wang, and Yun-Hui Liu. Neural markov random field for stereo matching. In *Proceedings of the IEEE/CVF Conference on Computer Vision and Pattern Recognition*, pages 5459–5469, 2024. 6
- [14] Xiaoyang Guo, Kai Yang, Wukui Yang, Xiaogang Wang, and Hongsheng Li. Group-wise correlation stereo network. In *Proceedings of the IEEE/CVF Conference on Computer Vision and Pattern Recognition*, pages 3273–3282, 2019. 2, 3, 5, 6, 8
- [15] Kaiming He, Xiangyu Zhang, Shaoqing Ren, and Jian Sun. Spatial pyramid pooling in deep convolutional networks for visual recognition. *IEEE transactions on pattern analysis and machine intelligence*, 37(9):1904–1916, 2015. 2
- [16] Byeongho Heo, Minsik Lee, Sangdoon Yun, and Jin Young Choi. Knowledge transfer via distillation of activation boundaries formed by hidden neurons. In *Proceedings of the AAAI conference on artificial intelligence*, pages 3779–3787, 2019. 3
- [17] Geoffrey Hinton. Distilling the knowledge in a neural network. *arXiv preprint arXiv:1503.02531*, 2015. 2, 3, 7, 8
- [18] Yiwen Hua, Puneet Kohli, Pritish Uplavikar, Anand Ravi, Saravana Gunaseelan, Jason Orozco, and Edward Li. Holopix50k: A large-scale in-the-wild stereo image dataset. *arXiv preprint arXiv:2003.11172*, 2020. 7
- [19] Junpeng Jing, Jiankun Li, Pengfei Xiong, Jiangyu Liu, Shuaicheng Liu, Yichen Guo, Xin Deng, Mai Xu, Lai Jiang, and Leonid Sigal. Uncertainty guided adaptive warping for robust and efficient stereo matching. In *Proceedings of the IEEE/CVF International Conference on Computer Vision*, pages 3318–3327, 2023. 3
- [20] Alex Kendall, Hayk Martirosyan, Saumitro Dasgupta, Peter Henry, Ryan Kennedy, Abraham Bachrach, and Adam Bry. End-to-end learning of geometry and context for deep stereo regression. In *Proceedings of the IEEE international conference on computer vision*, pages 66–75, 2017. 2, 3, 4, 5
- [21] Kisoo Kwon, Hwidong Na, Hoshik Lee, and Nam Soo Kim. Adaptive knowledge distillation based on entropy. In *ICASSP 2020-2020 IEEE International Conference on Acoustics, Speech and Signal Processing (ICASSP)*, pages 7409–7413. IEEE, 2020. 2, 3, 7
- [22] Jiankun Li, Peisen Wang, Pengfei Xiong, Tao Cai, Ziwei Yan, Lei Yang, Jiangyu Liu, Haoqiang Fan, and Shuaicheng Liu. Practical stereo matching via cascaded recurrent network with adaptive correlation. In *Proceedings of the IEEE/CVF Conference on Computer Vision and Pattern Recognition*, pages 16263–16272, 2022. 3
- [23] Lahav Lipson, Zachary Teed, and Jia Deng. Raft-stereo: Multilevel recurrent field transforms for stereo matching. In *2021 International Conference on 3D Vision (3DV)*, pages 218–227. IEEE, 2021. 3, 6
- [24] Biyang Liu, Huimin Yu, and Guodong Qi. Graftnet: Towards domain generalized stereo matching with a broad-spectrum and task-oriented feature. In *Proceedings of the IEEE/CVF Conference on Computer Vision and Pattern Recognition*, pages 13012–13021, 2022. 1, 2, 3, 6
- [25] Ce Liu, Suryansh Kumar, Shuhang Gu, Radu Timofte, Yao Yao, and Luc Van Gool. Stereo risk: A continuous modeling approach to stereo matching. In *Proceedings of the 41st International Conference on Machine Learning*, pages 31326–31343. PMLR, 2024. 6

- [26] Yufan Liu, Jiajiong Cao, Bing Li, Chunfeng Yuan, Weiming Hu, Yangxi Li, and Yunqiang Duan. Knowledge distillation via instance relationship graph. In *Proceedings of the IEEE/CVF Conference on Computer Vision and Pattern Recognition*, pages 7096–7104, 2019. 3
- [27] Nikolaus Mayer, Eddy Ilg, Philip Hausser, Philipp Fischer, Daniel Cremers, Alexey Dosovitskiy, and Thomas Brox. A large dataset to train convolutional networks for disparity, optical flow, and scene flow estimation. In *Proceedings of the IEEE conference on computer vision and pattern recognition*, pages 4040–4048, 2016. 1, 2, 5, 6, 7, 8
- [28] Moritz Menze and Andreas Geiger. Object scene flow for autonomous vehicles. In *Proceedings of the IEEE conference on computer vision and pattern recognition*, pages 3061–3070, 2015. 1, 2, 5, 6, 7
- [29] Zhibo Rao, Bangshu Xiong, Mingyi He, Yuchao Dai, Renjie He, Zhelun Shen, and Xing Li. Masked representation learning for domain generalized stereo matching. In *Proceedings of the IEEE/CVF Conference on Computer Vision and Pattern Recognition*, pages 5435–5444, 2023. 1, 6
- [30] Daniel Scharstein, Heiko Hirschmüller, York Kitajima, Greg Krathwohl, Nera Nešić, Xi Wang, and Porter Westling. High-resolution stereo datasets with subpixel-accurate ground truth. In *German conference on pattern recognition*, pages 31–42. Springer, 2014. 1, 2, 5, 6, 7
- [31] Thomas Schops, Johannes L Schonberger, Silvano Galliani, Torsten Sattler, Konrad Schindler, Marc Pollefeys, and Andreas Geiger. A multi-view stereo benchmark with high-resolution images and multi-camera videos. In *Proceedings of the IEEE Conference on Computer Vision and Pattern Recognition*, pages 3260–3269, 2017. 1, 2, 5, 6, 7
- [32] Zhelun Shen, Yuchao Dai, and Zhibo Rao. Cfnets: Cascade and fused cost volume for robust stereo matching. In *Proceedings of the IEEE/CVF Conference on Computer Vision and Pattern Recognition*, pages 13906–13915, 2021. 6
- [33] Z. Shen, Y. Dai, et al. Pcw-net: Pyramid combination and warping cost volume for stereo matching. In *ECCV*, 2022. 2, 3, 5, 6, 8
- [34] Zachary Teed and Jia Deng. Raft: Recurrent all-pairs field transforms for optical flow. In *Computer Vision—ECCV 2020: 16th European Conference, Glasgow, UK, August 23–28, 2020, Proceedings, Part II 16*, pages 402–419. Springer, 2020. 3
- [35] Fabio Tosi, Yiyi Liao, Carolin Schmitt, and Andreas Geiger. Smd-nets: Stereo mixture density networks. In *Proceedings of the IEEE/CVF Conference on Computer Vision and Pattern Recognition*, pages 8942–8952, 2021. 2, 3
- [36] Stepan Tulyakov, Anton Ivanov, and Francois Fleuret. Practical deep stereo (pds): Toward applications-friendly deep stereo matching. *Advances in neural information processing systems*, 31, 2018. 1, 2, 3, 5, 6, 7, 8
- [37] Meng-Chieh Wu, Ching-Te Chiu, and Kun-Hsuan Wu. Multi-teacher knowledge distillation for compressed video action recognition on deep neural networks. In *ICASSP 2019-2019 IEEE International Conference on Acoustics, Speech and Signal Processing (ICASSP)*, pages 2202–2206. IEEE, 2019. 2, 3
- [38] Gangwei Xu, Junda Cheng, Peng Guo, and Xin Yang. Attention concatenation volume for accurate and efficient stereo matching. In *Proceedings of the IEEE/CVF Conference on Computer Vision and Pattern Recognition*, pages 12981–12990, 2022. 2
- [39] Gangwei Xu, Xianqi Wang, Xiaohuan Ding, and Xin Yang. Iterative geometry encoding volume for stereo matching. In *Proceedings of the IEEE/CVF Conference on Computer Vision and Pattern Recognition*, pages 21919–21928, 2023. 1, 3, 6, 8
- [40] Peng Xu, Zhiyu Xiang, Chengyu Qiao, Jingyun Fu, and Tianyu Pu. Adaptive multi-modal cross-entropy loss for stereo matching. In *Proceedings of the IEEE/CVF Conference on Computer Vision and Pattern Recognition*, pages 5135–5144, 2024. 1, 2, 3, 5, 6, 7, 8
- [41] Lihe Yang, Bingyi Kang, Zilong Huang, Xiaogang Xu, Jiashi Feng, and Hengshuang Zhao. Depth anything: Unleashing the power of large-scale unlabeled data. In *Proceedings of the IEEE/CVF Conference on Computer Vision and Pattern Recognition*, pages 10371–10381, 2024. 1, 5
- [42] Chin-Chia Michael Yeh, Yan Zhu, Liudmila Ulanova, Nurjahan Begum, Yifei Ding, Hoang Anh Dau, Diego Furtado Silva, Abdullah Mueen, and Eamonn Keogh. Matrix profile i: all pairs similarity joins for time series: a unifying view that includes motifs, discords and shapelets. In *2016 IEEE 16th international conference on data mining (ICDM)*, pages 1317–1322. Ieee, 2016. 3
- [43] Shan You, Chang Xu, Chao Xu, and Dacheng Tao. Learning from multiple teacher networks. In *Proceedings of the 23rd ACM SIGKDD international conference on knowledge discovery and data mining*, pages 1285–1294, 2017. 2, 3, 7
- [44] Sergey Zagoruyko and Nikos Komodakis. Paying more attention to attention: Improving the performance of convolutional neural networks via attention transfer. *arXiv preprint arXiv:1612.03928*, 2016. 3
- [45] Feihu Zhang, Victor Prisacariu, Ruigang Yang, and Philip HS Torr. Ga-net: Guided aggregation net for end-to-end stereo matching. In *Proceedings of the IEEE/CVF Conference on Computer Vision and Pattern Recognition*, pages 185–194, 2019. 6
- [46] Feihu Zhang, Xiaojuan Qi, Ruigang Yang, Victor Prisacariu, Benjamin Wah, and Philip Torr. Domain-invariant stereo matching networks. In *European Conference on Computer Vision*, pages 420–439. Springer, 2020. 1, 3, 5, 6
- [47] Hailin Zhang, Defang Chen, and Can Wang. Confidence-aware multi-teacher knowledge distillation. In *ICASSP 2022-2022 IEEE International Conference on Acoustics, Speech and Signal Processing (ICASSP)*, pages 4498–4502. IEEE, 2022. 7
- [48] Jiawei Zhang, Xiang Wang, Xiao Bai, Chen Wang, Lei Huang, Yimin Chen, Lin Gu, Jun Zhou, Tatsuya Harada, and Edwin R Hancock. Revisiting domain generalized stereo matching networks from a feature consistency perspective. In *Proceedings of the IEEE/CVF Conference on Computer Vision and Pattern Recognition*, pages 13001–13011, 2022. 2, 3, 5, 6
- [49] Youmin Zhang, Yimin Chen, Xiao Bai, Suihanjin Yu, Kun Yu, Zhiwei Li, and Kuiyuan Yang. Adaptive unimodal cost

volume filtering for deep stereo matching. In *Proceedings of the AAAI Conference on Artificial Intelligence*, pages 12926–12934, 2020. [1](#), [2](#), [3](#)

- [50] Haoliang Zhao, Huizhou Zhou, Yongjun Zhang, Jie Chen, Yitong Yang, and Yong Zhao. High-frequency stereo matching network. In *Proceedings of the IEEE/CVF Conference on Computer Vision and Pattern Recognition*, pages 1327–1336, 2023. [3](#)